Prediction of shear capacity of steel channel sections using machine learning algorithms

Madhushan Dissanayake[a], Hoang Nguyen[a], Keerthan Poologanathan[a], Gatheeshgar Perampalam[a], Irindu Upasiri[b,*], Heshachanaa Rajanayagam[a], Thadshajini Suntharalingam[a]

[a]*Department of Mechanical and Construction Engineering, Northumbria University, Newcastle upon Tyne NE1 8ST, United Kingdom*
[b]*Faculty of Engineering, University of Sri Jayewardenepura, Ratmalana, Sri Lanka*

Abstract

This study presents the application of popular machine learning algorithms in prediction of the shear resistance of steel channel sections using experimental and numerical data. Datasets of 108 results of stainless steel lipped channel sections and 238 results of carbon steel LiteSteel sections were gathered to train machine learning models including support vector regression (SVR), multi-layer perceptron (MLP), gradient boosting regressor (GBR), and extreme gradient boosting (XGB). The cross-validation with 10 folds has been conducted in the training process to avoid over-fitting. The optimal hyperparameter combinations for each machine learning model were found during the hyperparameter tuning process and four performance indicators were used to evaluate the performance of the trained models. The comparison results suggest that all four implemented machine learning models reliably predict the shear capacity of both stainless steel lipped channel sections and carbon steel LiteSteel sections while the implemented SVR algorithm is found to be the best performing model. Moreover, it is shown that the implemented machine learning models exceed the prediction accuracy of the available design equations in estimating the shear capacity of steel channel sections.

Keywords: Channel sections, Shear capacity, Design rules, Machine learning

*Corresponding author.
Email address: irinduupasiri@gmail.com (Irindu Upasiri)

1. Introduction

Light gauge cold-formed steel elements have gained interest over heavier hot-rolled sections in recent times as cost effective, highly efficient structural solutions [1]. Szewczak et al. [2] reported that the use of thin-walled steel sections have reduced the steel consumption by up to 50%, construction time by up to 60% and construction costs by up to 25%, compared to conventional hot-rolled sections. Cold-formed lipped channel beams (LCBs) and LiteSteel beams (LSBs) are most utilised as primary and secondary load-carrying structural elements such as roof purlins, wall studs, steel framing, truss beams, and floor joists and bearers [1, 3–5].

Stainless steel is an evolving cold-forming material in the construction industry due to its outstanding material properties. Higher chromium content in stainless steel acts as a protective layer against oxidation and corrosion [6–8]. The unique characteristics that cold-formed stainless steel sections feature include corrosion resistance, fire and heat resistance, durability, good toughness and fatigue properties, high strength to weight ratio, simple fabrication and handling, and recyclability [4, 8]. The application of stainless steel in the construction industry has been increased with the improved insight of its advantages such as savings from corrosion-resistant coatings, reduced inspection frequency, maintenance, downtime and replacement costs, and a transition towards sustainability. However, stainless steel has become less popular in structural applications due to the high initial material cost of stainless steel structural components when compared to carbon steel. Therefore, the accurate prediction of resistance of stainless steel sections is of paramount importance.

Many research studies have been conducted to investigate the shear performance of cold-formed channel sections in the recent past, both experimentally and numerically. Keerthan and Mahendran [9, 10] performed experimental studies on the shear behaviour of carbon steel LSBs and LCBs, and the shear design equations have been proposed based on North American specifications [11]. Furthermore, Keerthan and Mahendran [1, 12, 13] developed finite element (FE) models to predict the non-linear shear behaviour of carbon steel channels, including their elastic buckling and ultimate shear capacities with precision. In addition, Pham and Hancock [14–17] conducted both experimental and numerical investigations on the shear response of plain and stiffened carbon steel channel sections. Since there was an absence of comprehensive investigations on the shear behaviour of cold-formed stainless steel LCBs to date, Dissanayake et al. [18] performed a combined experimental and numerical study to predict the shear behaviour and strength of stainless steel LCBs. Dissanayake et al. [19] also conducted FE investigations to assess the shear and elastic shear buckling behaviours of the longitudinally stiffened stainless steel LCBs. Ishqy et al. [6] studied the effect of unreinforced circular web openings on the shear behaviour of cold-formed stainless steel LCBs numerically. Moreover, Sonu and Singh [20, 21] examined the shear performance of lean duplex stainless steel rectangular hollow beams using FE analyses. These studies involve the modification of existing design rules considering the inelastic reserve capacity and strain hardening effect of stainless steel to enhance the shear capacity prediction accuracy of European standards for stainless steel [22] and the Direct Strength Method (DSM).

In recent years, the artificial intelligence methods, especially machine learning, have gained a lot of attention in civil engineering applications by offering viable solutions for complex problems such as prediction, classification and optimisation [23]. It is evident that the utilization of machine learning in civil engineering has fuelled many visions and hopes for future research and development [24–26]. The machine learning methods can perform exceptionally well in prediction the non-linear relationships among the inputs and outputs which are difficult to formulate otherwise and do not necessarily require large amount of data [24]. Also, the machine learning models are computationally efficient and at the same time can be expandable to provide robust predictions even with large amount of data. The application of machine learning has been featured in numerous civil and structural engineering research publications [26–29].

The machine learning prediction models have been utilised in many civil and structural engineering research areas. Fonseca et al. [30] have investigated the possibility of employing experimental and numerical data to train an artificial neural network (ANN) to predict the patch load resistance. The ANN models have also been developed using finite element data to predict the deflections for composite beams by Sakr and Sakla [31] and for steel-concrete composite bridges by Tadesse et al. [32]. A particle swarm optimization-based neural network was proposed to predict the failure of multi-storied reinforced concrete buildings by Chatterjee et al. [33]. Abdollahzadeh and Ghobadi [34] proposed a neural network model to predict the hysteretic behaviour of perforated steel plate shear walls. The neural network-based models were also developed using finite element data to estimate the stress concentration factors for multi-planar tubular joints by Chiew et al. [35] and for welded joints by Dabiri et al. [36, 37]. The computational prediction models including genetic programming were developed using test results for moment-rotation behaviour of boltless steel connections by Shah et al. [38]. In another study, Bağcı [39] predicted the moment-curvature relationship of reinforced concrete sections using ANN. Jakubek [40] trained multi-layer perceptron and fuzzy weights neural network models to predict the load capacity of eccentrically loaded reinforced concrete columns. Naderpour et al. [41] used different soft computing methods for the compressive strength prediction of FRP-confined reinforced concrete columns. Hadi [42] conducted optimization studies on concrete beams using back-propagation neural networks. The use of single and ensemble machine learning methods in prediction of long-term deflections of reinforced concrete beams were investigated by Pham et al. [43]. Erdem [44] applied the ANNs to predict the moment capacity of reinforced concrete slabs in fire. McKinney and Ali [45] have employed supervised ANNs in spalling classification and failure prediction of high strength concrete columns subjected to fire. Also, a genetic algorithm optimized back-propagation neural network was developed for the determination of flexural capacity of postfire reinforced concrete beams by Cai et al. [46]. Moreover, Shen et al. [47] have proposed a new material design method for ultra-high strength stainless steel using machine learning algorithms. And Mu et al. [48] have devised an ensemble machine learning model to predict the strain-induced martensite in austenitic steels. Vu et al. [49] have proposed an efficient framework based on the gradient tree boosting algorithms for the strength prediction of the concrete filled steel tubular columns. A gradient tree boosting model was also used by Truong et al. [50] to evaluate the safety of steel trusses through prediction of the load-carrying capacity and the displacement of the structure. Kim et al. [51] have assessed the efficiency of different machine learning models to predict and classify the load-carrying resistance of steel frames. It is of note that the most of these applications of machine learning models have outperformed the existing design methods in providing accurate predictions.

The use of machine learning prediction models in these particular application fields is explained by the availability of the large quantity of initial data on which the learning algorithm or the network is trained and most of the above applications provide reasonably easy access to large datasets, for example, through repeated laboratory experiments or computer modelling [52]. In addition, the application of machine learning models in civil engineering has dealt with structural health monitoring, damage detection of structures, structural optimization, and structural parameter identification. The structural health monitoring and material property modelling of concrete have received significant attention in the recent past among these machine learning applications in civil engineering [24]. The machine learning algorithms have also been used to classify the failure modes of ultra-high performance concrete beams [53]. Fig. 1 illustrates the typical workflow of machine learning processes.

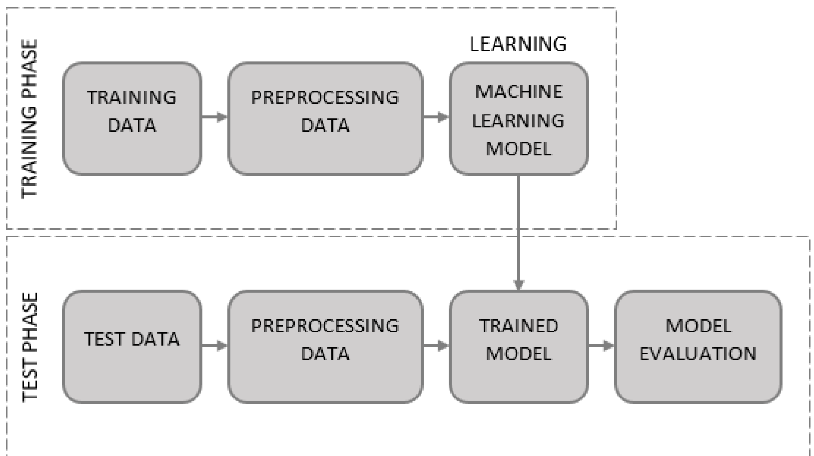

Figure 1: Typical workflow of machine learning processes.

In terms of tackling structural engineering problems, especially in order to analyse the structural behaviours, data-driven approaches have been used. To estimate material properties, researchers have established predictive models which minimise the prediction error between the actual data collected from experiments and models [54]. Machine learning applications typically use classification and prediction to solve problems. As machine learning enables training of algorithms and testing them based on available datasets, the mastery of models, basic statistics and availability of reliable data are essential to make most accurate predictions [25].

Although many past studies have utilised machine learning prediction models for design and performance prediction of reinforced concrete and hot-rolled steel structures, there are very few articles which focus on the application of machine learning to predict the behaviour of cold-formed sections. In particularly, past studies have not attempted to investigate the application of machine learning models in prediction of the shear strength of cold-formed stainless steel and carbon steel channel sections. The accurate determination of section strengths plays vital role in planning and design of steel structures. The available machine learning models can be easily implemented to handle large number of data to make robust predictions. Therefore, considering the benefits of using machine learning prediction models in structural design, this research study aims to analyse the applicability of machine learning in prediction of the shear capacity of cold-formed stainless steel LCBs and carbon steel LSBs to develop efficient machine learning prediction tools which will potentially help to lower the costs associated with experiments and FE simulations.

2. The development of database

A database of compiled results is required for the successful implementation of machine learning algorithms. Hence, a literature survey has been undertaken to collect the results from experimental and FE studies on the shear capacity of cold-formed stainless steel and carbon steel beams. This section presents a brief review of experimental and FE modelling methods used herein followed by a summary of the collected database.

2.1. Overview of experimental and FE analysis

Dissanayake et al. [18] and Keerthan and Mahendran [9, 12] have investigated the shear behaviour of cold-formed stainless steel LCBs and cold-formed carbon steel LSBs, respectively. The cross-sections of a LCB section and a LSB section are illustrated in Fig. 2. The aspect ratio, which is defined as the clear shear span (a) divided by the clear web height (d_1), governs the shear failure. It is considered that a shear dominant failure occurs when this ratio is equal to unity. For stainless steel LCB sections, Dissanayake et al.'s [18] test programme included aspect ratio of 1.0 while for LSB sections, Keerthan and Mahendran's [9] test programme included aspect ratio of 1.0 and 1.5. Three-point loading test arrangement with two shear spans was used in both studies. The shear capacity was found from the peak load of the load-displacement response. More details about the three-point loading test programmes of cold-formed sections can be found from similar experimental studies [10, 15, 16, 55]. These experimental studies have been further extended using validated FE models.

Keerthan and Mahendran [12] and Dissanayake et al. [18] have developed non-linear FE models in the advanced FE modelling software, ABAQUS [56].

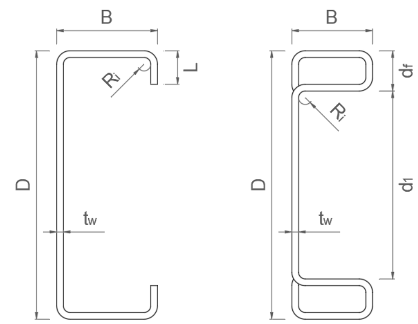

Figure 2: Cross-sections of LCB and LSB sections with key dimensions.

The developed FE models were validated against the experimental results in terms of shear capacity, failure mode and load-displacement response. Subsequently, parametric FE analysis was performed changing the dimensional and mechanical parameters. The S4R shell elements available in ABAQUS [56] element library were used to develop the FE model components of both the steel channel section and the web side plates. The web side plates were modelled with shell elements and a higher thickness value was assigned to simulate the rigid body behaviour. These web side plates were connected using tie constraints option. A mesh size of 5 mm $\times$ 5 mm was employed to flat parts and a mesh size of 1 mm $\times$ 5 mm was employed to corner parts of the channel sections. Meanwhile, a coarser mesh size was assigned to the web side plates as the shear behaviour of the channel is not influenced by the web side plates. Fig. 3 depicts the FE mesh and boundary conditions employed in the FE models for LCBs.

The accurate material modelling of cold-formed carbon steel and stainless steel is required to obtain the actual behaviour from the FE model. The stress-strain response of carbon steel was taken as a bi-linear model with perfect plasticity using nominal yield strength. However, stainless steel exhibits a considerable degree of strain hardening as well as strength enhancements due to cold-working. Therefore, the material model proposed by Arrayago et al. [57], which is based on the modified Ramberg-Osgood model, was used. The strength enhancements were assigned to the corner regions of the model as per the Cruise and Gardner's [58] recommendations. Moreover, the initial geometric imperfections were considered in the FE model superimposing the critical elastic buckling analysis modes. An illustration of obtained FE shear failure mode for LCB is also displayed in Fig. 3. For further details related

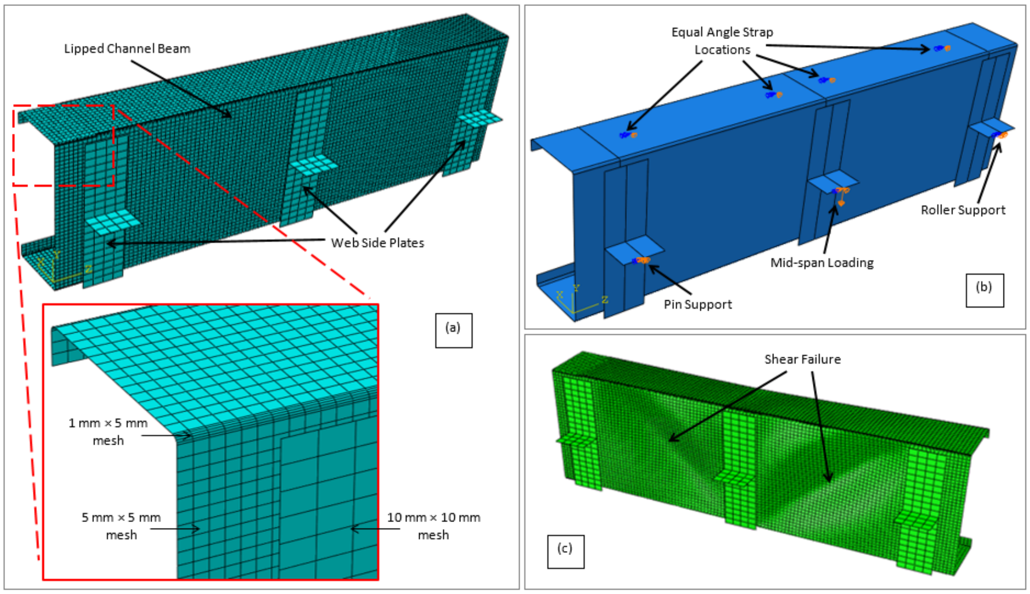

Figure 3: FE modelling of LCB section: (a) Mesh, (b) Boundary conditions, and (c) Failure mode.

to the FE modelling of cold-formed sections, similar numerical work can be referred [1, 13, 14, 17, 19, 59–61].

2.2. Collected datasets

Dissanayake et al. [18] and Keerthan and Mahendran [9, 12] have generated a wide range of data using experimental and FE analysis methods as described in the previous section. All the related data from their studies were collated to form a database with input and output features. The details of the collected data are discussed herein.

For cold-formed stainless steel LCB sections, 108 results were collected in total from Dissanayake et al.'s [18] study. This includes 8 shear test results and 100 numerical parametric study results. The dataset consists of various geometric and material parameters as input features. The considered geometric input features of stainless steel LCBs include web depth (D), flange width (B), lip height (L), and web thickness (t_w). Also, aspect ratio (a/d_1) and a slenderness measure of the web (d_1/t_w) are taken into account. The adopted material property features include the yield strength (f_y) and the ultimate strength (f_u) of stainless steel. And, the output feature is the shear strength (V) of LCBs. Table 1 reports the key statistics of input and output features of LCBs dataset.

Table 1: Key statistics of cold-formed stainless steel LCBs dataset

	#samples		D (mm)	B (mm)	L (mm)	t_w (mm)	a/d_1	d_1/t_w	f_y (MPa)	f_u (MPa)	V (kN)
Experiment	8	Min	99.48	50.0	15.5	1.18	1.0	45.97	253.9	725.3	18.5
		Max	200.98	75.5	16.5	1.99	1.0	163.55	253.9	725.3	47.1
FE	100	Min	100.0	50.0	15.0	1.0	1.0	17.2	230.0	540.0	12.93
		Max	250.0	75.0	15.0	5.0	1.0	244.0	500.0	700.0	356.07
Overall	108	Min	99.48	50.0	15.0	1.0	1.0	17.2	230.0	540.0	12.93
		Max	250.0	75.5	16.5	5.0	1.0	244.0	500.0	725.3	356.07

The gathered stainless steel LCBs dataset covers a range of parameters that can be seen in practice. For an instance, the depth of the LCBs ranges from 99.48 mm to 250 mm. The thickness of the LCBs is varying between 1 mm and 5 mm. The minimum and maximum values of the average yield strength of the LCBs are 230 MPa and 500 MPa, respectively. Meanwhile, the corresponding ultimate strength values range from 540 MPa to 725.3 MPa.

For cold-formed carbon steel LSB sections, 238 results were collected in total including 25 shear test results and 213 parametric FE results from the respective studies [9, 12]. Similar to the previously discussed LCBs dataset, the considered geometric dimensions of LSBs include web depth (D), flange width (B), clear web height (d_1), and web thickness (t_w). In addition, it considers aspect ratio (a/d_1) and a slenderness parameter of the web (d_1/t_w). The yield strength (f_y) of carbon steel is the only material property considered. Similarly, the shear strength (V) of LSBs is taken as the output feature. The key statistics of input and output features of LSBs dataset are summarised in Table 2.

As can be seen, Table 2 also demonstrates that the collated dataset covers a full spectrum of practically used LSB sections in light gauge steel construction. For an instance, the depth of the LSBs ranges from 125 mm to 300 mm. The thickness of the LSBs is varying between 1.5 mm and 3 mm. The minimum and maximum values of the average yield strength of the LSBs from the collected data are 250 MPa and 459.7 MPa, respectively.

It is also of note that both the collected stainless steel and carbon steel datasets cover the elastic and inelastic shear buckling, and shear yielding failure behaviours. Furthermore, both datasets include a wide range of com-

Table 2: Key statistics of cold-formed carbon steel LSBs dataset

	#samples		D (mm)	B (mm)	d_1 (mm)	t_w (mm)	a/d_1	d_1/t_w	f_y (MPa)	V (kN)
Experiment	25	Min	125.0	45.0	95.2	1.58	1.0	49.07	422.6	45.8
		Max	300.0	75.0	262.3	2.51	1.6	133.14	459.7	143.7
FE	213	Min	150.0	45.0	119.7	1.5	1.0	60.0	250.0	29.8
		Max	300.0	75.0	260.8	3.0	1.5	163.0	450.0	173.0
Overall	238	Min	125.0	45.0	95.2	1.5	1.0	49.07	250.0	29.8
		Max	300.0	75.0	262.3	3.0	1.6	163.0	459.7	173.0

mercially available cross-sectional dimensions and material grades covering a range of cross-section slenderness values and strengths. Therefore, the collected database is found to be handy in developing machine learning algorithms that could be more promising than the existing code provisions to predict the shear capacities of stainless steel LCBs and carbon steel LSBs.

3. Review of design equations for cold-formed sections

The currently available design provisions for cold-formed sections are reviewed in this section. The shear design equations given in European standards for stainless steel, EN1993-1-4 [22] and the direct strength method (DSM) shear provisions in North American specifications for cold-formed steel members, AISI S100 [11] have been modified by Dissanayake et al. [18] to enhance the shear resistance prediction accuracy of cold-formed stainless steel LCBs. Also, Keerthan and Mahendran [12] have revised the DSM shear design provisions in AISI S100 [11] considering the cold-formed carbon steel LSBs. These proposed design provisions are found to be more accurate than the codified design provisions. Therefore, the revised provisions were adopted and would be used to compare and assess the prediction performance of the machine learning models in Section 5.

3.1. EN1993-1-4 shear design rules

European standards for stainless steel, EN1993-1-4 [22] provide a separate set of shear design equations which are to be referred together with European standards for plated steel elements, EN1993-1-5 [62]. Following these standards, the shear resistance of a section ($V_{b,Rd}$) is taken as the summation of the shear buckling resistance of the section web ($V_{bw,Rd}$) and the flange contribution to the shear resistance of the section ($V_{bf,Rd}$) as follows

$$V_{b,Rd} = V_{bw,Rd} + V_{bf,Rd} \leq \frac{\eta f_{yw} h_w t_w}{\sqrt{3}\gamma_{M1}}, \tag{1}$$

where f_{yw} is the yield strength of the section web, h_w is the web depth, and t_w is the web thickness. γ_{M1} is the partial safety factor and a value of $\eta = 1.2$ is recommended. The shear buckling resistance of the section web ($V_{bw,Rd}$) can be calculated as

$$V_{bw,Rd} = \frac{\chi_w f_{yw} h_w t_w}{\sqrt{3}\gamma_{M1}}, \tag{2}$$

where χ_w is the shear buckling reduction factor of the web. EN1993-1-4 [22] provides a separate set of expressions for this shear buckling reduction factor (χ_w) of section webs with rigid end posts and they are expressed as follows

$$\chi_w = \eta \qquad \text{for } \bar{\lambda}_w \leq \frac{0.65}{\eta}, \tag{3a}$$

$$\chi_w = \frac{0.65}{\bar{\lambda}_w} \qquad \text{for } \frac{0.65}{\eta} < \bar{\lambda}_w < 0.65, \tag{3b}$$

$$\chi_w = \frac{1.56}{0.91 + \bar{\lambda}_w} \qquad \text{for } \bar{\lambda}_w \geq 0.65, \tag{3c}$$

where $\bar{\lambda}_w$ is the slenderness of the section web.

Following a number of experimental and numerical studies on cold-formed stainless steel LCBs, Dissanayake et al. [18] have proposed a modification to Eq. (3) to increase the prediction accuracy. These modified expressions are expressed as follows

$$\chi_w = 2.1 \qquad \text{for } \bar{\lambda}_w \leq 0.12, \tag{4a}$$

$$\chi_w = \frac{0.839}{\bar{\lambda}_w^{0.433}} \qquad \text{for } 0.12 < \bar{\lambda}_w < 0.667, \tag{4b}$$

$$\chi_w = \frac{1.797}{1.13 + \bar{\lambda}_w} \qquad \text{for } \bar{\lambda}_w \geq 0.667. \tag{4c}$$

3.2. The direct strength method (DSM)

The DSM has been adopted in North American specifications for cold-formed steel members, AISI S100 [11]. The nominal shear strength of a section (V_n) with transverse web stiffeners are given as follows

$$\frac{V_n}{V_y} = 1 \qquad \text{for } \lambda \leq 0.776, \tag{5a}$$

$$\frac{V_n}{V_y} = \left[1 - 0.15\left(\frac{1}{\lambda^2}\right)^{0.4}\right]\left(\frac{1}{\lambda^2}\right)^{0.4} \qquad \text{for } \lambda > 0.776, \tag{5b}$$

where λ is the section slenderness.

Dissanayake et el. [18] have also modified the DSM design equations given by Eq. (5) considering stainless steel LCBs. The modified DSM equations for the section nominal shear strength are expressed as follows

$$\frac{\mathrm{V_n}}{\mathrm{V_y}} = 2 \qquad \text{for } \lambda \leq 0.122, \tag{6a}$$

$$\frac{\mathrm{V_n}}{\mathrm{V_y}} = \frac{0.795}{\lambda^{0.439}} \qquad \text{for } 0.122 < \lambda \leq 0.592, \tag{6b}$$

$$\frac{\mathrm{V_n}}{\mathrm{V_y}} = \left[1 - 0.213\left(\frac{1}{\lambda^2}\right)^{0.35}\right]\left(\frac{1}{\lambda^2}\right)^{0.35} \qquad \text{for } \lambda > 0.592. \tag{6c}$$

In addition, extensive experimental and numerical investigations have been conducted by Keerthan and Mahendran [9, 12] on cold-formed carbon steel LSB sections. Based on these investigations, Keerthan and Mahendran [12] have revised the DSM shear design equations given by Eq. (5) aiming enhanced resistance predictions. The proposed DSM equations for the nominal shear strength of sections are stated as follows

$$\frac{V_n}{V_y} = 1 \qquad \text{for } \lambda \leq 0.815, \tag{7a}$$

$$\frac{V_n}{V_y} = \left[1 - 0.15\left(\frac{1}{\lambda^2}\right)^{0.5}\right]\left(\frac{1}{\lambda^2}\right)^{0.5} \qquad \text{for } \lambda > 0.815. \tag{7b}$$

4. Machine learning algorithms

4.1. Overview

In this study, four well-known machine learning algorithms including support vector machine (SVM), multi-layer perceptron (MLP), and gradient boosting machine (GBM) are used to predict the shear capacities of stainless LCBs and carbon steel LSBs. This section aims to provide a brief overview of these models and the details of the implementation process of these models in application to collected datasets.

4.1.1. Support vector machine

SVMs are categorised as supervised learning algorithms and can be utilised for classification and regression problems. Vapnik and his team [63, 64] have immensely contributed to the development of SVMs in the last decades. When applying these SVMs in solving regression related problems, it is known as support vector regression (SVR).

The fundamental concept behind SVMs is the non-linear mapping of the input vectors into a high dimensional feature space where the linear decision surface is constructed. The generalisation ability of the learning machine is ensured through the properties of the decision surface [64].

In other words, considering a set of training data $\{(x_1, y_1), (x_2, y_2), ...,$ $(x_n, y_n)\} \subset \chi \times \mathbb{R}$, the aim of ϵ-SVR [63] is to predict a flat decision function, $f(x)$ such that $f(x)$ is only allowed to deviate from the actual data y_i in the range of $(-\epsilon, \epsilon)$ for all the data in the training set [65]. For the case of linear decision function, $f(x)$ this can be expressed as

$$f(x) = \langle \omega, x \rangle + b \quad \text{with} \quad \omega \in \chi, \quad b \in \mathbb{R}, \tag{8}$$

where ω and b represent the weight and bias, respectively.

However, finding a decision function is not always possible as there could be data points in some datasets that are lying outside the feasible region [64, 65]. To address this issue, Cortes and Vapnik [64] have considered the "soft margin" loss function in SVMs and therefore slack variables ξ_i are introduced as illustrated in Fig. 4a. Then, setting the objective of flattening the decision function leads to the formulation of the optimisation problem that includes the slack variables ξ_i as follows [63]

$$\begin{aligned} \text{minimize} \quad & \frac{1}{2}\|\omega\|^2 + C\sum_{i=1}^{n}(\xi_i), && \text{(9a)} \\ \text{subject to} \quad & |y_i - \langle \omega, x \rangle - b| \leq \epsilon + \xi_i, && \text{(9b)} \\ & \xi_i \geq 0, && \text{(9c)} \\ & C > 0, && \text{(9d)} \end{aligned}$$

where C determines both the flatness of the decision function $f(x)$ and the limit of the deviations that are larger than ϵ.

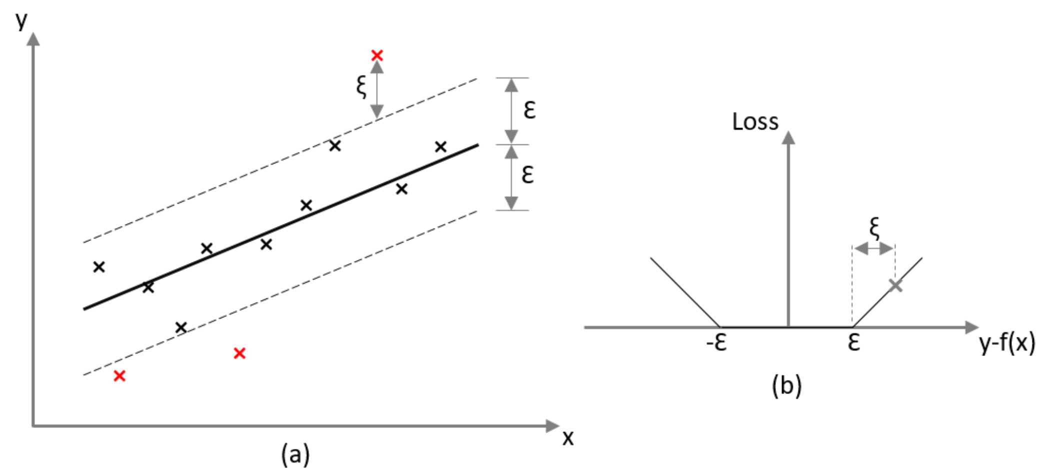

Figure 4: (a) "Soft margin" for linear SVM and (b) ϵ-insensitive loss function.

Only the points which deviate more than ϵ from the function contribute to the loss function in a linear fashion. This is known as ϵ-insensitive loss function $|\xi|_\epsilon$ [65] and this loss function which is illustrated in Fig. 4b is defined as

$$|\xi|_\epsilon = \begin{cases} 0 & \text{if } \xi \leq \epsilon, \\ \xi - \epsilon & \text{otherwise.} \end{cases} \tag{10}$$

Moreover, non-linear functions are introduced to SVM algorithms with the help of a kernel function when the linear decision function is no longer feasible. The kernel function defines the mapping of the training data from a lower dimensional feature space to a higher dimensional feature space. To achieve this, different types of kernel functions are employed [64, 65].

4.1.2. Multi-layer perceptron

MLP network is a feed-forward artificial neural network (ANN) which consists of layers of interconnected nodes. The layer with input features is named as input layer followed by one or more hidden layers and finally an output layer with one or more target outputs. Each layer consists of number of nodes known as neurons. The neurons are interconnected between layers [66]. The connection between two adjacent layers neurons are called weights

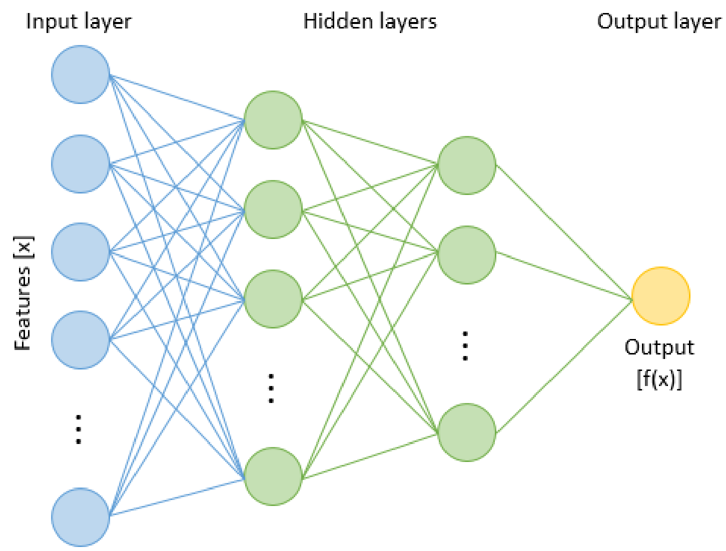

Figure 5: A multi-layer neural network with two hidden layers and a single output.

and biases are attached to each neuron. A multi-layer neural network with two hidden layers and a single output is illustrated in Fig. 5.

The input layer consists all the input features and feeds them to the network. Each neuron in hidden layers sends and output signal to the next layer in the form of a weighted linear summation modified by a non-linear transfer function known as activation function [67]. The output a_i of the i^{th} neuron in a particular hidden layer passed on to the next layer is defined as follows

$$a_i = f\left(\sum_{j=1}^{n}(w_{ij}a_j + b_i)\right), \tag{11}$$

where $f()$ is the activation function, w_{ij} is the weight between the j^{th} neuron in the previous layer and i^{th} neuron in the current layer, a_j is the output of the j^{th} neuron in the previous layer, and b_i is the bias of the i^{th} neuron in the current layer.

There are many different types of activation functions available. These includes linear, sigmoid, tanh and rectified linear units (ReLU) [67]. Finally, the output layer transforms the values received from hidden layers into outputs.

MLP networks can be trained to learn the mapping function between the input vector and the output vector using a set of training data. During the training process, an output is first obtained based on the initially assumed weights and biases when a training data set is presented to the network. Then, the error signal is calculated comparing the difference between the target and obtained outputs. This error signal is back-propagated through the network, and weights and biases are adjusted to minimise the overall error. A technique known as gradient descent is used to find the global minimum point on the error surface during the iterative training process [67].

4.1.3. Gradient boosting machine

GBMs are the ensemble models combining weak, base-learners in a sequential manner to minimise the overall error of the whole ensemble. Friedman [68] has first developed these boosting method in 1999. In GBMs, decision or regression trees are employed as base learners. During the learning process, a new weak, base learner is added to the model at the each iteration step. The new weak, base learner is trained to reduce the overall error of the ensemble at that point [69]. The sequential adding of new base learners is repeated until a desirable accuracy is achieved. This step by step addition of decision trees to the ensemble model at the each iteration to reduce the overall error to form a strong tree ensemble model is illustrated from Fig. 6.

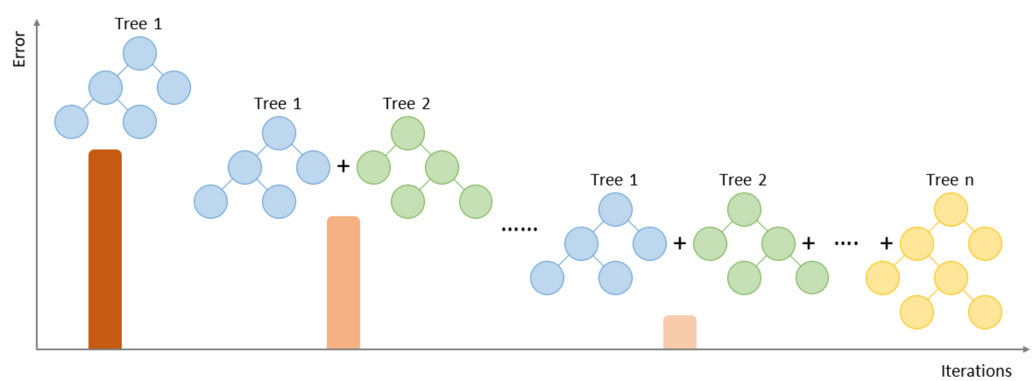

Figure 6: Gradient tree boosting machines.

In GBMs the error of the ensemble model is also known as the loss function. A number of loss functions are supported by GBMs and sometimes a case specific loss functions can be implemented [69]. Consider a vector input $x = \{x_1, x_2, ..., x_n\}$ and its output y. The output is dependent of input through function f. The aim of GBM algorithm is to find an estimated function $F(x)$ between inputs and the respective output such that the loss function $\Psi(y, f)$ is minimised. This can be expressed as follows

$$F(x) = \arg\min_{f(x)} \Psi(y, f(x)) . \tag{12}$$

In the ensemble model, the step-wise addition of the function in the iterative process for N number of iterations is given as

$$F_N(x) = \sum_{i=0}^{N} F_i(x), \tag{13}$$

where the initial estimation is $F_0(x)$.

When it comes to regression problems, gradient boosting regressor (GBR) and extreme gradient boosting (XGB) algorithms can be applied. The importance of XGB is that its high-scalability and at the same time, it performs more efficiently compared to other common boosting models [70].

4.2. Model implementation

Four machine learning models including SVR, MLP, GBR, and XGB were implemented in Python for the shear resistance prediction of considered steel sections. The implementation has been expanded from the codes provided by Nguyen et al. [54] which was based on popular open source machine learning libraries including `scikit-learn` [71] and `XGBoost` [70]. The details of data pre-processing, cross-validation, and hyperparameter tuning are briefed in this section.

4.2.1. Pre-processing of data

The pre-processing of data before it is being utilised for the training of a particular model is vital. One aspect of data pre-processing is to normalise the data into a uniform scale. The idea behind this is to avoid any domination and numerical difficulty associated with large numerals during the training phase of the model. In this study, all the input features were normalised to the scale of 0 to 1. Then, the normalised input features were used to train the models and the predicted outputs were transformed back to the original scale for testing.

4.2.2. Cross-validation

The traditional approaches of cross-validation sometimes lead to overfitting of the model in the training phase. The K-fold cross-validation method has been introduced to overcome this problem. Kohavi [72] has shown that choosing 10 number of folds provides the best results within a reasonable time. This approach has also been used in a number of published works [54, 73, 74]. Therefore, 10-fold cross-validation has been utilised in this study.

In the 10-fold cross-validation, the dataset is randomly divided into ten folds with approximately equal size. Then, while keeping one fold as the test set, the remaining nine folds are used for the training set. Once the first training is finished, in the next round, another fold is used as the test set, while remaining nine folds are used for the training. The process is repeated ten times to ensure that each fold is considered as the test set for one time and is contributed to the training set nine times. The final performance of the model is reported by taking the mean of ten training and testing rounds. This process of 10-fold cross-validation is illustrated in Fig. 7.

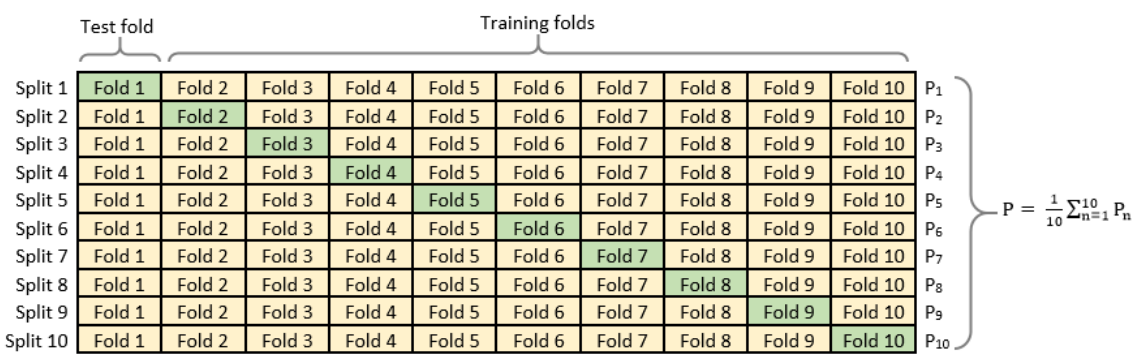

Figure 7: Cross-validation with ten folds.

4.2.3. Hyperparameter tuning

The performance of the most of the machine learning models is sensitive to the values of their hyperparameters [75–77]. During the hyperparameter tuning process, the optimal values for each hyperparameter are identified through the implemented machine learning algorithms. First, a set of values is predefined for each hyperparameter. Then, the values are assigned to the each hyperparameter from the predefined sets to form different hyperparameter combinations. Thereafter, the machine learning model is trained and evaluated for each of the hyperparameter combination, and the best performing combination is found during the tuning.

5. Prediction results and discussion

The performance of the developed machine learning models are evaluated using four performance indicators and then the performance of machine learning algorithms are compared with the currently available design equations presented in Section 3.

5.1. Performance indicators

To evaluate the performance of different prediction approaches of shear capacity of steel channel sections including the implemented machine learning algorithms and design equations, four performance indicators were incorporated in this study. These four indicators are linear correlation coefficient (R), root mean square error (RMSE), mean absolute error (MAE), and mean absolute percentage error (MAPE).

To calculate the linear correlation coefficient R, the coefficient of determination R^2 shall be determined as follows

$$R^2 = 1 - \frac{\sum^{n}(y-\hat{y})^2}{\sum^{n}(y-\bar{y})^2}, \tag{14}$$

where y denotes the actual data and $\hat{y}$ represents the predicted value. $\bar{y}$ corresponds to the mean value of the actual data and n is the size of the data sample. It is considered to be a good prediction, if the linear correlation coefficient R is closer to 1.

Other performance indicators RMSE, MAE, and MAPE can be determined as follows

$$\text{RMSE} = \sqrt{\frac{1}{n}\sum^{n}(y-\hat{y})^2}, \tag{15a}$$

$$\text{MAE} = \frac{1}{n}\sum^{n}|y-\hat{y}|, \tag{15b}$$

$$\text{MAPE} = \frac{1}{n}\sum^{n}\left|\frac{y-\hat{y}}{y}\right| \times 100. \tag{15c}$$

The lower values of RMSE, MAE, and MAPE suggest that the error is less, therefore a better prediction.

5.2. *Performance of the machine learning models*

5.2.1. *Cold-formed stainless steel LCBs*

Table 3 summarises the identified optimal combination of some hyperparameters during the hyperparameter tuning process for each machine learning algorithm while Table 4 compares the performance of each algorithm using four performance indicators discussed above for the cold-formed stainless steel LCB sections. As can be seen from Table 4, all four algorithms demonstrate good performances in prediction of shear capacity of stainless steel LCBs and the implemented SVR machine learning model provides the best performance among four algorithms in all indicators.

Table 3: Hyperparameter combinations of machine learning algorithms in prediction of shear capacity of stainless steel LCBs

Method	Hyperparameter				
SVR	`kernel`	`C`	`epsilon`	`gamma`	-
	'rbf'	600	0.01	0.1	-
MLP	`hidden_layer_sizes`	`solver`	`max_iter`	`alpha`	-
	(100,60)	'lbfgs'	900	0.0001	-
GBR	`n_estimators`	`max_depth`	`learning_rate`	`loss`	`min_samples_split`
	1000	10	0.1	'lad'	10
XGB	`n_estimators`	`max_depth`	`learning_rate`	`objective`	-
	1400	2	0.35	'reg:linear'	-

Table 4: The performance of machine learning algorithms in prediction of shear capacity of stainless steel LCBs

Method	R	RMSE (kN)	MAE (kN)	MAPE (%)
SVR	0.999	2.76	2.32	4.03
MLP	0.998	4.13	3.18	5.95
GBR	0.997	5.53	4.19	4.47
XGB	0.997	5.51	4.31	6.86

The experimental and FE shear capacities of stainless steel LCBs are compared with the machine learning predictions for SVR and MLP models in Figs. 8 and 9, respectively. It can be seen that the model predictions are distributed closer to the actual data line and also the scatter of the predictions

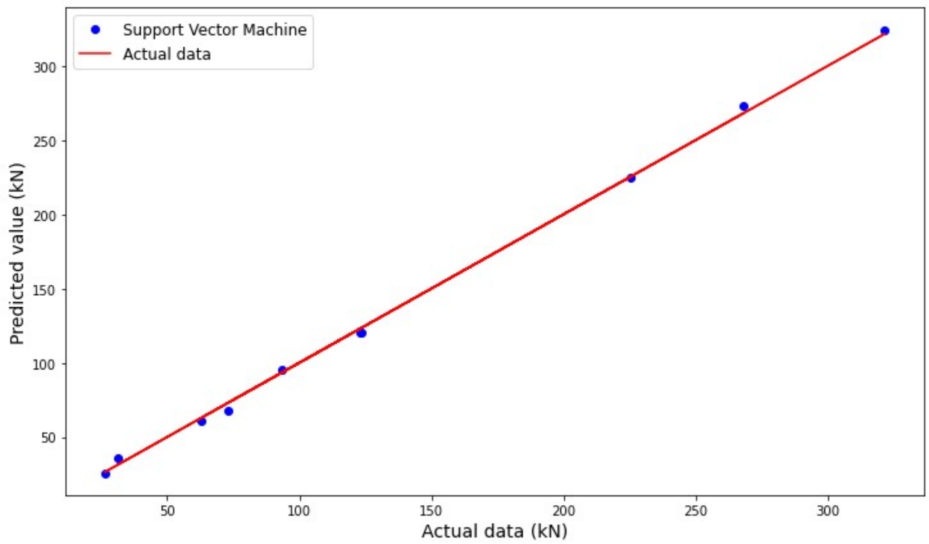

Figure 8: Performance of SVR model in prediction of shear capacity of stainless steel LCBs.

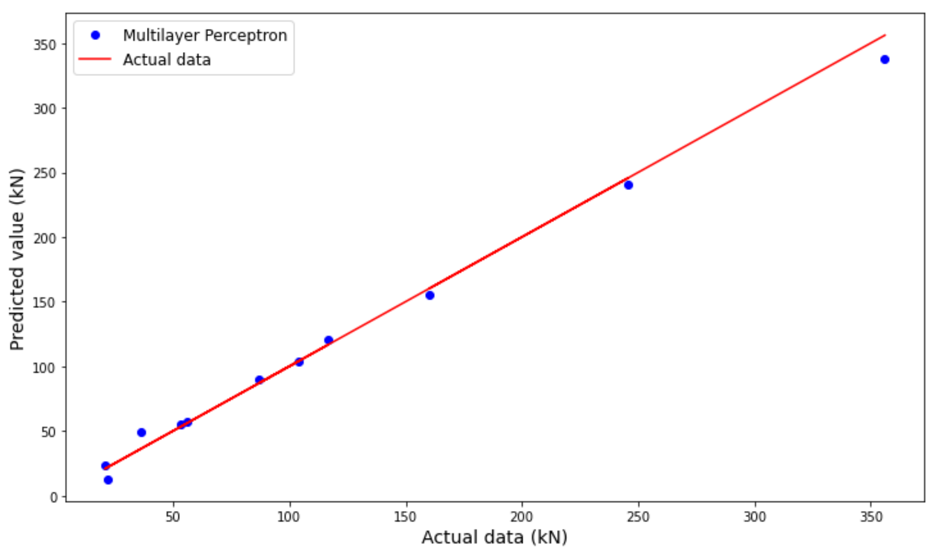

Figure 9: Performance of MLP model in prediction of shear capacity of stainless steel LCBs.

is very low. Therefore, the accuracy of machine learning predictions is further evidenced from these comparisons.

The relative importance of each input feature on the shear strength of the section was evaluated using the XGBoost library [70]. A higher value of relative feature importance implies that the impact of the particular input feature on the output is more significant. Fig. 10 illustrates the relative importance of each input feature on the shear strength of stainless steel LCB sections. From the figure, it can be observed that the input features yield strength f_y, web thickness t_w and section depth D have a considerably higher impact on the shear strength while yield strength f_y is being the most dominant among all features. On the other hand, a relatively lower feature importance can be seen from the features d_1/t_w, flange width B and lip height L. Interestingly, the ultimate strength f_u and aspect ratio have the least impact on the shear strength. There is no variation of aspect ratio in the input data set could be the reason for the lower rank of the feature in the relative importance. Also, the considered sections could have gained the shear strength before reaching the ultimate stress and therefore, this could result in ranking the ultimate strength f_u low.

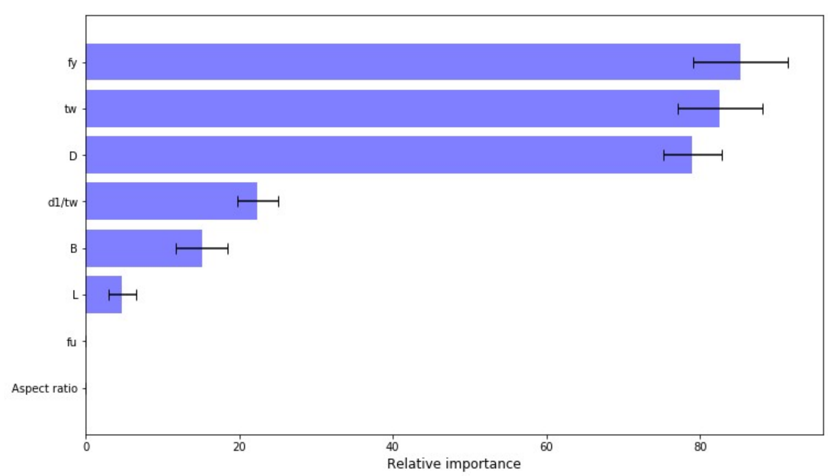

Figure 10: Relative importance of input features on the shear capacity of stainless steel LCBs.

5.2.2. Cold-formed carbon steel LSBs

The hyperparameter combinations which give the best predictions and the performance indicators of four machine learning algorithms are summarised for the cold-formed carbon steel LSBs in Tables 5 and 6, respectively. The comparison results reported in Table 6 suggest that all four machine learning models are able to perform well in prediction of shear capacity of carbon steel LSBs as well. The implemented SVR model again offers the best agreement considering the overall performance.

Table 5: Hyperparameter combinations of machine learning algorithms in prediction of shear capacity of carbon steel LSBs

Method	Hyperparameter				
SVR	`kernel`	`C`	`epsilon`	`gamma`	-
	'rbf'	600	0.01	0.3	-
MLP	`hidden_layer_sizes`	`solver`	`max_iter`	`alpha`	-
	(300,100)	'lbfgs'	350	0	-
GBR	`n_estimators`	`max_depth`	`learning_rate`	`loss`	`min_samples_split`
	1500	4	0.15	'huber'	6
XGB	`n_estimators`	`max_depth`	`learning_rate`	`objective`	-
	800	2	0.15	'reg:linear'	-

Table 6: The performance of machine learning algorithms in prediction of shear capacity of carbon steel LSBs

Method	R	RMSE (kN)	MAE (kN)	MAPE (%)
SVR	0.999	1.26	0.95	1.43
MLP	0.998	1.65	1.05	1.39
GBR	0.997	2.19	1.49	1.89
XGB	0.996	2.06	1.35	1.74

Figs. 11 and 12 illustrate the comparison of experimental and FE shear strengths of carbon steel LSBs with the machine learning predictions for SVR and MLP algorithms, respectively. The distribution and lower scatter of predictions demonstrate a good agreement with actual data.

Fig. 13 is produced to evaluate the relative importance of considered input features on the shear strength of carbon steel LSB sections. The illustration indicates that the feature yield strength f_y has the highest influence on the shear strength of carbon steel LSBs which is a little less than twice of the importance of the second most influencing feature web thickness t_w. In contrast, the flange width B is found to be the feature with the least impact.

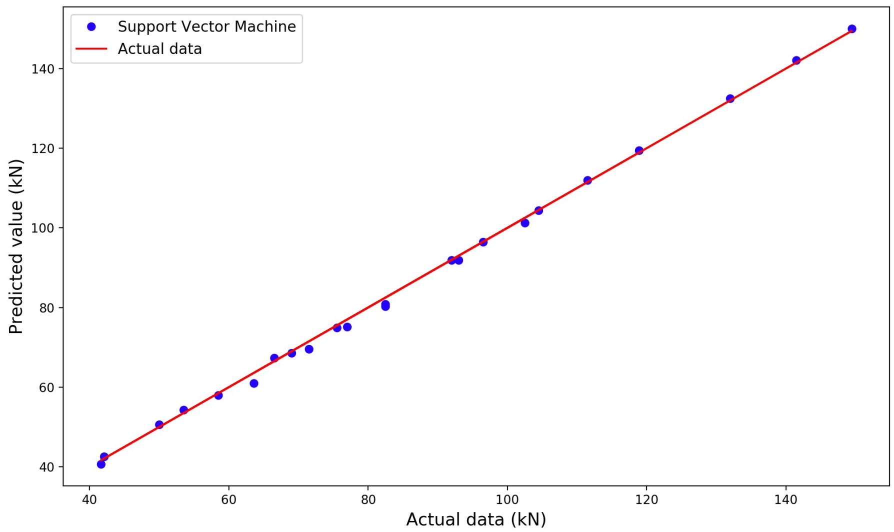

Figure 11: Performance of SVR model in prediction of shear capacity of carbon steel LSBs.

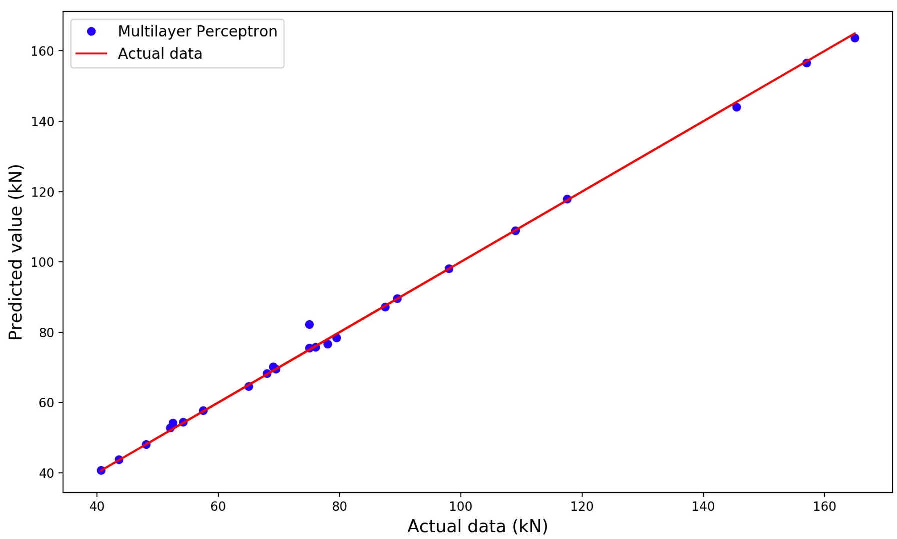

Figure 12: Performance of MLP model in prediction of shear capacity of carbon steel LSBs.

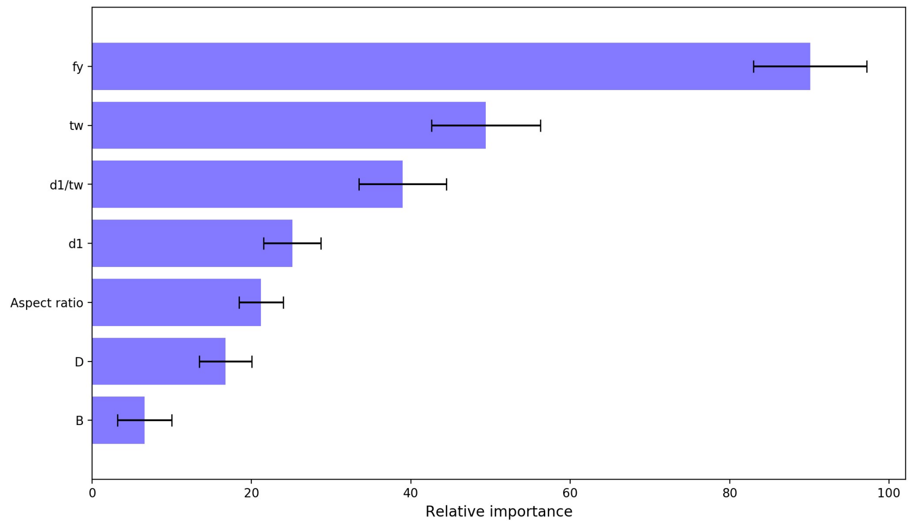

Figure 13: Relative importance of input features on the shear capacity of carbon steel LSBs.

5.3. Performance of the design equations

The performance of the design equations was also evaluated in prediction of shear capacity of stainless steel LCBs and carbon steel LSBs using four performance indicators. The modified shear design provisions for EN1993-1-4 [22] in Eq. (4) and the proposed DSM shear design equations in Eqs. (6-7) were incorporated herein.

Table 7 summarises the calculated performance indicators of these design equations for both stainless steel and carbon steel databases considered in this study. It can be observed that all four performance indicators provide fairly satisfactory results in prediction of shear strength of LCBs and LSBs using design equations.

Table 7: Performance of design equations in prediction of shear capacities of LCBs and LSBs

Problem	Design equation	R	RMSE (kN)	MAE (kN)	MAPE (%)
LCB	Eq. (4) [18]	0.998	3.78	2.85	3.56
	Eq. (6) [18]	0.998	4.16	3.29	4.28
LSB	Eq. (7) [12]	0.979	6.21	4.71	6.01

Furthermore, the experimental and FE shear capacities are compared with the design equation predictions. Figs. 14-16 present the comparisons for Eq. (4), Eq. (6), and Eq. (7). The predictions of the best performing machine learning model which is SVR are also included in these comparisons.

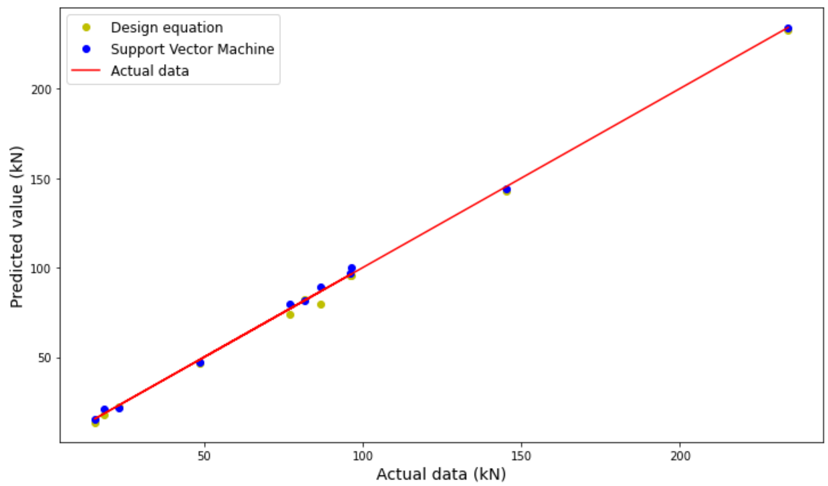

Figure 14: Comparison of the performance of Eq. (4) and SVR model in prediction of shear capacity of stainless steel LCBs.

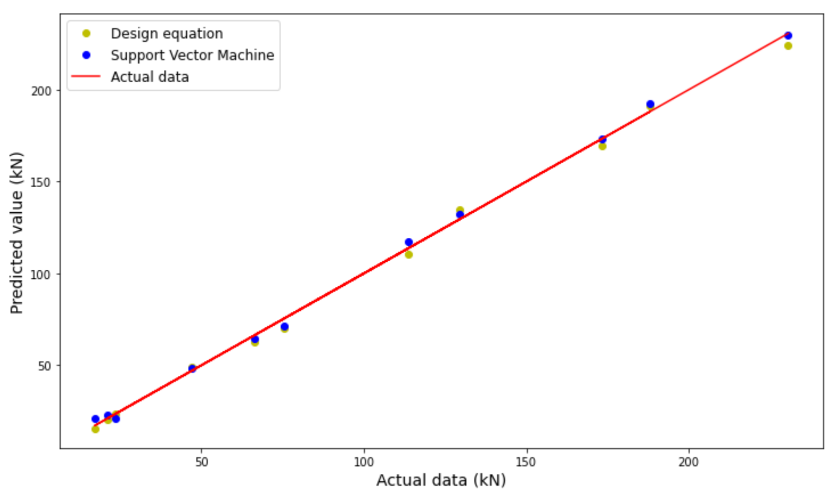

Figure 15: Comparison of the performance of Eq. (6) and SVR model in prediction of shear capacity of stainless steel LCBs.

It can be observed from Figs. 14 and 15 that the distribution and the scatter of design equation predictions for stainless steel LCBs are marginally

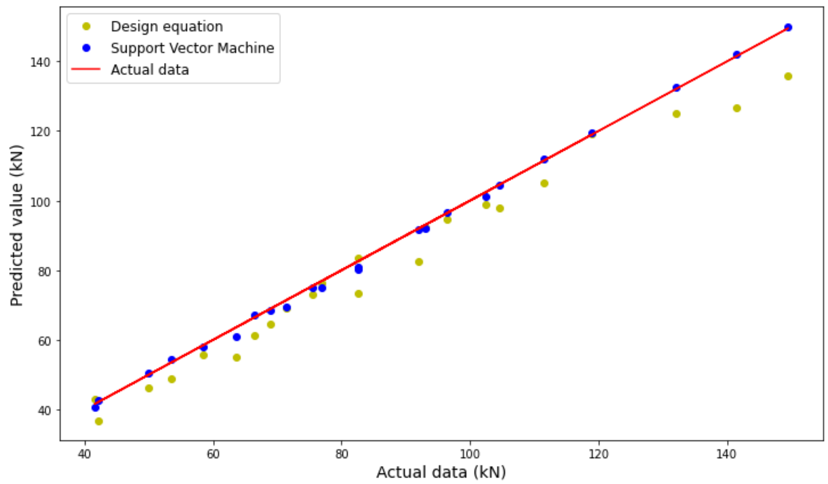

Figure 16: Comparison of the performance of Eq. (7) and SVR model in prediction of shear capacity of carbon steel LSBs.

equal to that of SVR model. However, the performance indicators are still found to be better when machine learning models are used. Additionally, Fig. 16 shows that the design equation predictions for carbon steel LSBs are deviated away from the actual data line with a considerably higher scatter than SVR model predictions. The design equation predictions appear to be slightly conservative for LSBs.

Therefore, the comparison suggests that the implemented four machine learning algorithms (SVR, MLP, GBR, and XGB) can be employed in accurate prediction of the shear capacity of steel channel sections. Even though, the existing design rules also seem to provide accurate predictions for the shear capacity, the improvement of machine learning predictions compared to the design rules can still be seen from the considered four performance indicators. In contrast to the available experimental and numerical methods which require greater deal of resources, the machine learning algorithms can be easily implemented as a tool in the decision making process to help civil or structural engineers. This study highlights the availability of machine learning as an efficient and powerful tool, which can be implemented for accurate prediction of any section resistance of interest, given that adequate number of previous data is available.

6. Concluding remarks

This study presents the application of popular machine learning algorithms in prediction of the shear resistance of steel channel sections. The experimental and numerical results of three-point loading tests of cold-formed stainless steel LCBs and carbon steel LSBs are gathered from previous studies and then employed in training machine learning algorithms. Support vector regression, multi-layer perceptron, gradient boosting regressor, and extreme gradient boosting algorithms were implemented in the study to predict the shear capacity of steel channel sections using 108 results of LCBs and 238 results of LSBs. During the implementation of algorithms, pre-processing of data, 10-fold cross-validation and hyperparameter tuning were performed. The optimal hyperparameter combinations for each machine learning model were found and the performance of the developed machine learning models were evaluated based on performance indicators including linear correlation coefficient, root mean square error, mean absolute error, and mean absolute percentage error. Then, the performance of machine learning algorithms were compared with the design equations predictions.

The developed SVR, MLP, GBR, and XGB machine learning models are efficient and predicted well the shear capacity of both stainless steel LCBs and carbon steel LSBs. The implemented SVR algorithm is proved to be the best performing model in this study. Moreover, the evaluated performance indicators for the design equations suggest fairly satisfactory results giving conservative predictions. The implemented machine learning algorithms are found to be performing better than the available design equations in prediction of the shear capacities of stainless steel LCBs and carbon steel LSBs. Therefore, this study highlights the applicability of machine learning algorithms to solve similar structural and civil engineering problems when carefully prepared data is present.

References

[1] P. Keerthan, M. Mahendran, Improved shear design rules of cold-formed steel beams, Engineering Structures 99 (2015) 603–615.

[2] I. Szewczak, K. Rzeszut, P. Rozylo, Structural behaviour of steel cold-formed sigma beams strengthened with bonded steel tapes, Thin-Walled Structures 159 (2021) 107295.

[3] M.-T. Chen, B. Young, A. D. Martins, D. Camotim, P. B. Dinis, Experimental investigation on cold-formed steel lipped channel beams affected by local-distortional interaction under non-uniform bending, Thin-Walled Structures 161 (2021) 107494.

[4] N. Baddoo, Stainless steel in construction: A review of research, applications, challenges and opportunities, Journal of Constructional Steel Research 64 (11) (2008) 1199–1206, international Stainless Steel Experts Seminar.

[5] L. Gardner, The use of stainless steel in structures, Progress in Structural Engineering and Materials 7 (2) (2005) 45–55.

[6] M. F. M. Ishqy, S. Wanniarachchi, K. Poologanathan, S. Gunalan, P. Gatheeshgar, T. Suntharalingam, S. Navaratnam, Shear behaviour of cold-formed stainless-steel beams with web openings: Numerical studies, Structures 31 (2021) 127–144.

[7] SCI, Design Manual for Structural Stainless Steel, Fourth edition, 4th Edition, The Steel Construction Institute, Ascot, UK, 2017.

[8] B. Rossi, Discussion on the use of stainless steel in constructions in view of sustainability, Thin-Walled Structures 83 (2014) 182–189.

[9] P. Keerthan, M. Mahendran, Experimental studies on the shear behaviour and strength of litesteel beams, Engineering Structures 32 (10) (2010) 3235 – 3247.

[10] P. Keerthan, M. Mahendran, Experimental investigation and design of lipped channel beams in shear, Thin-Walled Structures 86 (2015) 174–184.

[11] AISI-S100–16, North American Specification for the Design of Cold-Formed Steel Structural Members, American Iron and Steel Institute (AISI), 2016.

[12] P. Keerthan, M. Mahendran, New design rules for the shear strength of litesteel beams, Journal of Constructional Steel Research 67 (6) (2011) 1050 – 1063.

[13] P. Keerthan, M. Mahendran, Numerical modeling of litesteel beams subject to shear, Journal of Structural Engineering 137 (12) (2011) 1428–1439.

[14] C. H. Pham, G. J. Hancock, Numerical simulation of high strength cold-formed purlins in combined bending and shear, Journal of Constructional Steel Research 66 (10) (2010) 1205–1217.

[15] C. H. Pham, G. J. Hancock, Direct strength design of cold-formed c-sections for shear and combined actions, Journal of Structural Engineering 138 (6) (2012) 759–768.

[16] C. H. Pham, L. A. Bruneau, G. J. Hancock, Experimental study of longitudinally stiffened web channels subjected to combined bending and shear, Journal of Structural Engineering 141 (11) (2015) 04015018.

[17] C. H. Pham, G. J. Hancock, Numerical investigation of longitudinally stiffened web channels predominantly in shear, Thin-Walled Structures 86 (2015) 47–55.

[18] D. Dissanayake, K. Poologanathan, S. Gunalan, K. Tsavdaridis, B. Nagaratnam, K. Wanniarachchi, Numerical modelling and shear design rules of stainless steel lipped channel sections, Journal of Constructional Steel Research 168 (2020) 105873.

[19] D. Dissanayake, K. Poologanathan, S. Gunalan, K. Tsavdaridis, K. Wanniarachchi, B. Nagaratnam, Numerical investigation of cold-formed stainless steel lipped channels with longitudinal stiffeners subjected to shear, Thin-Walled Structures 158 (2021) 107179.

[20] J. Sonu, K. D. Singh, Shear characteristics of lean duplex stainless steel (ldss) rectangular hollow beams, Structures 10 (2017) 13–29.

[21] J. Sonu, K. D. Singh, Shear behaviour of single perforated lean duplex stainless steel (ldss) rectangular hollow beams, Thin-Walled Structures 119 (2017) 851–867.

[22] EN1993-1-4:2006+A1:2015, Eurocode 3 – Design of Steel Structures – Part 1–4: General Rules – Supplementary Rules for Stainless Steels, European Committee for Standardization (CEN), 2015.

[23] C. Graciano, A. E. Kurtoglu, E. Casanova, Machine learning approach for predicting the patch load resistance of slender austenitic stainless steel girders, Structures 30 (2021) 198–205.

[24] H. Salehi, R. Burgueño, Emerging artificial intelligence methods in structural engineering, Engineering Structures 171 (2018) 170–189.

[25] S. Mitra, Applications of machine learning and computer vision for smart infrastructure management in civil engineering, Master's thesis, University of New Hampshire, Durham, US, master's Thesis (2017).

[26] H. Adeli, Neural networks in civil engineering: 1989–2000, Computer-Aided Civil and Infrastructure Engineering 16 (2) (2001) 126–142.

[27] R. Vanluchene, R. Sun, Neural networks in structural engineering, Computer-Aided Civil and Infrastructure Engineering 5 (3) (1990) 207–215.

[28] I. Flood, N. Kartam, T. Tongthong, The application of artificial neural networks to civil engineering, in: Computing in Civil Engineering, ASCE, 1994, pp. 668–675.

[29] P. Lu, S. Chen, Y. Zheng, Artificial intelligence in civil engineering, Mathematical Problems in Engineering 2012 (2012) 145974.

[30] E. T. Fonseca, P. C. d. S. Vellasco, S. A. de Andrade, M. M. Vellasco, A patch load parametric analysis using neural networks, Journal of Constructional Steel Research 59 (2) (2003) 251–267.

[31] M. A. Sakr, S. S. Sakla, Long-term deflection of cracked composite beams with nonlinear partial shear interaction—a study using neural networks, Engineering structures 31 (12) (2009) 2988–2997.

[32] Z. Tadesse, K. Patel, S. Chaudhary, A. Nagpal, Neural networks for prediction of deflection in composite bridges, Journal of Constructional Steel Research 68 (1) (2012) 138–149.

[33] S. Chatterjee, S. Sarkar, S. Hore, N. Dey, A. S. Ashour, V. E. Balas, Particle swarm optimization trained neural network for structural failure prediction of multistoried rc buildings, Neural Computing and Applications 28 (8) (2017) 2005–2016.

[34] G. Abdollahzadeh, F. Ghobadi, Linked mathematical–informational modeling of perforated steel plate shear walls, Thin-Walled Structures 94 (2015) 512–520.

[35] S. Chiew, A. Gupta, N. Wu, Neural network-based estimation of stress concentration factors for steel multiplanar tubular xt-joints, Journal of Constructional Steel Research 57 (2) (2001) 97–112.

[36] M. Dabiri, M. Ghafouri, H. R. Raftar, T. Björk, Utilizing artificial neural networks for stress concentration factor calculation in butt welds, Journal of Constructional Steel Research 138 (2017) 488–498.

[37] M. Dabiri, M. Ghafouri, H. R. Raftar, T. Björk, Neural network-based assessment of the stress concentration factor in a t-welded joint, Journal of Constructional Steel Research 128 (2017) 567–578.

[38] S. Shah, N. R. Sulong, A. El-Shafie, New approach for developing soft computational prediction models for moment and rotation of boltless steel connections, Thin-Walled Structures 133 (2018) 206–215.

[39] M. Bağcı, Neural network model for moment-curvature relationship of reinforced concrete sections, Mathematical and Computational Applications 15 (1) (2010) 66–78.

[40] M. Jakubek, Neural network prediction of load capacity for eccentrically loaded reinforced concrete columns, Computer Assisted Methods in Engineering and Science 19 (4) (2017) 339–349.

[41] H. Naderpour, K. Nagai, P. Fakharian, M. Haji, Innovative models for prediction of compressive strength of frp-confined circular reinforced concrete columns using soft computing methods, Composite Structures 215 (2019) 69–84.

[42] M. N. Hadi, Neural networks applications in concrete structures, Computers & Structures 81 (6) (2003) 373–381.

[43] A.-D. Pham, N.-T. Ngo, T.-K. Nguyen, Machine learning for predicting long-term deflections in reinforce concrete flexural structures, Journal of Computational Design and Engineering 7 (1) (2020) 95–106.

[44] H. Erdem, Prediction of the moment capacity of reinforced concrete slabs in fire using artificial neural networks, Advances in Engineering Software 41 (2) (2010) 270–276.

[45] J. McKinney, F. Ali, Artificial neural networks for the spalling classification & failure prediction times of high strength concrete columns, Journal of Structural Fire Engineering 5 (3) (2014) 203–214.

[46] B. Cai, G.-l. Pan, F. Fu, Prediction of the postfire flexural capacity of rc beam using ga-bpnn machine learning, Journal of Performance of Constructed Facilities 34 (6) (2020) 04020105.

[47] C. Shen, C. Wang, X. Wei, Y. Li, S. van der Zwaag, W. Xu, Physical metallurgy-guided machine learning and artificial intelligent design of ultrahigh-strength stainless steel, Acta Materialia 179 (2019) 201–214.

[48] W. Mu, M. Rahaman, F. L. Rios, J. Odqvist, P. Hedström, Predicting strain-induced martensite in austenitic steels by combining physical modelling and machine learning, Materials and Design 197 (2021) 109199.

[49] Q.-V. Vu, V.-H. Truong, H.-T. Thai, Machine learning-based prediction of cfst columns using gradient tree boosting algorithm, Composite Structures 259 (2021) 113505.

[50] V.-H. Truong, Q.-V. Vu, H.-T. Thai, M.-H. Ha, A robust method for safety evaluation of steel trusses using gradient tree boosting algorithm, Advances in Engineering Software 147 (2020) 102825.

[51] S.-E. Kim, Q.-V. Vu, G. Papazafeiropoulos, Z. Kong, V.-H. Truong, Comparison of machine learning algorithms for regression and classification of ultimate load-carrying capacity of steel frames, Steel and Composite Structures 37 (2020) 193–209.

[52] B. D'Amico, R. Myers, J. Sykes, E. Voss, B. Cousins-Jenvey, W. Fawcett, S. Richardson, A. Kermani, F. Pomponi, Machine learning for sustainable structures: A call for data, in: Structures, Vol. 19, Elsevier, 2019, pp. 1–4.

[53] R. Solhmirzaei, H. Salehi, V. Kodur, M. Naser, Machine learning framework for predicting failure mode and shear capacity of ultra high performance concrete beams, Engineering Structures 224 (2020) 111221.

[54] H. Nguyen, T. Vu, T. P. Vo, H.-T. Thai, Efficient machine learning models for prediction of concrete strengths, Construction and Building Materials 266 (2021) 120950.

[55] P. Keerthan, D. Hughes, M. Mahendran, Experimental studies of hollow flange channel beams subject to combined bending and shear actions, Thin-Walled Structures 77 (2014) 129–140.

[56] ABAQUS, Analysis User's Guide 6.14, Dassault Systèmes Simulia Corp., Rhode Island, USA, 2014.

[57] I. Arrayago, E. Real, L. Gardner, Description of stress–strain curves for stainless steel alloys, Materials and Design 87 (2015) 540–552.

[58] R. B. Cruise, L. Gardner, Strength enhancements induced during cold forming of stainless steel sections, Journal of Constructional Steel Research 64 (11) (2008) 1310–1316, international Stainless Steel Experts Seminar.

[59] P. Keerthan, M. Mahendran, D. Hughes, Numerical studies and design of hollow flange channel beams subject to combined bending and shear actions, Engineering Structures 75 (2014) 197–212.

[60] D. Dissanayake, C. Zhou, K. Poologanathan, S. Gunalan, K. Tsavdaridis, J. Guss, Numerical simulation and design of stainless steel hollow flange beams under shear, Journal of Constructional Steel Research 176 (2021) 106414.

[61] D. Dissanayake, K. Poologanathan, S. Gunalan, K. Tsavdaridis, K. Wanniarachchi, B. Nagaratnam, Bending-shear interaction of cold-formed stainless steel lipped channel sections, Structures 30 (2021) 1042–1055.

[62] EN1993-1-5, Eurocode 3 – Design of Steel Structures – Part 1–5: Plated Structural Elements, European Committee for Standardization (CEN), 2006.

[63] V. Vapnik, The Nature of Statistical Learning Theory, Springer, 1995.

[64] C. Cortes, V. Vapnik, Support-vector networks, Machine Learning 20 (1995) 273–297.

[65] A. J. Smola, B. Schölkopf, A tutorial on support vector regression, Statistics and Computing 14 (2004) 199–222.

[66] M. H. Hassoun, et al., Fundamentals of artificial neural networks, MIT press, 1995.

[67] M. Gardner, S. Dorling, Artificial neural networks (the multilayer perceptron)—a review of applications in the atmospheric sciences, Atmospheric Environment 32 (14) (1998) 2627–2636.

[68] J. H. Friedman, Greedy function approximation: A gradient boosting machine., The Annals of Statistics 29 (5) (2001) 1189 – 1232.

[69] A. Natekin, A. Knoll, Gradient boosting machines, a tutorial, Frontiers in neurorobotics 7 (2013) 21.

[70] T. Chen, C. Guestrin, Xgboost: A scalable tree boosting system, in: Proceedings of the 22nd acm sigkdd international conference on knowledge discovery and data mining, 2016, pp. 785–794.

[71] F. Pedregosa, G. Varoquaux, A. Gramfort, V. Michel, B. Thirion, O. Grisel, M. Blondel, P. Prettenhofer, R. Weiss, V. Dubourg, J. Vanderplas, A. Passos, D. Cournapeau, M. Brucher, M. Perrot, E. Duchesnay, Scikit-learn: Machine learning in Python, Journal of Machine Learning Research 12 (2011) 2825–2830.

[72] R. Kohavi, A study of cross-validation and bootstrap for accuracy estimation and model selection, in: IJCAI, Vol. 14, Montreal, Canada, 1995, pp. 1137–1145.

[73] D.-K. Bui, T. Nguyen, J.-S. Chou, H. Nguyen-Xuan, T. D. Ngo, A modified firefly algorithm-artificial neural network expert system for predicting compressive and tensile strength of high-performance concrete, Construction and Building Materials 180 (2018) 320–333.

[74] V. V. Degtyarev, Neural networks for predicting shear strength of cfs channels with slotted webs, Journal of Constructional Steel Research 177 (2021) 106443.

[75] I. Goodfellow, Y. Bengio, A. Courville, Deep learning, Vol. 1, MIT press Cambridge, 2016.

[76] J. Bergstra, Y. Bengio, Random search for hyper-parameter optimization., Journal of machine learning research 13 (2) (2012).

[77] P. Probst, A.-L. Boulesteix, B. Bischl, Tunability: Importance of hyperparameters of machine learning algorithms., J. Mach. Learn. Res. 20 (53) (2019) 1–32.